Clinical Cancer Research

Perioperative Dynamic Changes in Circulating Tumor DNA in Patients with Lung Cancer (DYNAMIC)

Kezhong Chen[1], Heng Zhao[1], Yanbin Shi[2], Fan Yang[1], Lien Tu Wang[2], Guannan Kang[1], Yuntao Nie[1], and Jun Wang[1]

Abstract

Purpose: No study has investigated the precise perioperative dynamic changes in circulating tumor DNA (ctDNA) in any patients with early-stage cancer. This study (DYNAMIC) investigated perioperative dynamic changes in ctDNA and determined the appropriate detection time of ctDNA-based surveillance for surgical patients with lung cancer.

Experimental Design: Consecutive patients who underwent curative-intent lung resections were enrolled prospectively (NCT02965391). Plasma samples were obtained at multiple prespecified time points including before surgery (time A), during surgery after tumor resection (time B–time D), and after surgery (time P1–time P3). Next-generation sequencing–based detection platform was performed to calculate the plasma mutation allele frequency. The primary endpoint was ctDNA half-life after radical tumor resection.

Results: Thirty-six patients showed detectable mutations in time A. The plasma ctDNA concentration showed a rapid decreasing trend after radical tumor resection, with the average mutant allele fraction at times A, B, C, and D being 2.72%, 2.11%, 1.14%, and 0.17%, respectively. The median ctDNA half-life was 35.0 minutes. Patients with minimal residual disease (MRD) detection had a significant slower ctDNA half-life than those with negative MRD (103.2 minutes vs. 29.7 minutes, $P = 0.001$). The recurrence-free survival of patients with detectable and undetectable ctDNA concentrations at time P1 was 528 days and 543 days, respectively ($P = 0.657$), whereas at time P2 was 278 days and 637 days, respectively ($P = 0.002$).

Conclusions: ctDNA decays rapidly after radical tumor resection. The ctDNA detection on the third day after R0 resection can be used as the baseline value for postoperative lung cancer surveillance.

Introduction

Circulating tumor DNA (ctDNA) are short DNA fragments providing a comprehensive view of the tumor as were shed by tumor cells from multiple tumor regions (1). Application of ctDNA analysis has shown its clinical value for detecting molecular profiling, monitoring disease progress, and predicting treatment response in patients with advanced stage cancer (1–3). A few studies have also proved that in patients with early-stage cancer, the detection of ctDNA may reveal minimal residual disease (MRD) and identify patients who may be at higher risk of relapse (4–6). However, few study investigated the half-life of ctDNA in patients with cancer (7). Lo and colleagues investigated the clearance of circulating fetal DNA after delivery by using quantitative PCR analysis and showed that the mean half-life for circulating fetal DNA was 16.3 minutes (8); they also investigated the median half-life of plasma Epstein–Barr virus DNA after surgical resection was 139 minutes (9). Nevertheless, in patients with cancer, the mechanism of DNA clearance from plasma is poorly understood and it is not known how surgery influences ctDNA release and clearance; whether the presence of ctDNA after surgery is due to MRD or incomplete vanishment is unclear (10). No criteria have been established regarding the appropriate time for ctDNA detection as postoperative surveillance, confounding data interpretations, and the practical use of ctDNA in clinics (11).

Therefore, we designed this prospective cohort study (Dynamic/PTHO1602) to investigate perioperative dynamic changes in ctDNA in surgical patients with lung cancer. With the accurate monitoring of ctDNA levels before, during, and after surgery, we explored the half-life of ctDNA and the most suitable time for MRD detection.

Materials and Methods

Study design and participants

Consecutive patients with suspected lung cancers and intent to undergo curative surgery were enrolled prospectively. All patients had chest CT scans, abdominal and adrenal gland ultrasonograms or CT scans, brain MR images, and bone scans before surgery. PET/CT was not mandatory in every patient. Eligible patients were aged >18 years with no distant

[1]Department of Thoracic Surgery, Peking University People's Hospital, Beijing, China. [2]Berry Oncology Co., Ltd., Fujian, China.

Note: Supplementary data for this article are available at Clinical Cancer Research Online (http://clincancerres.aacrjournals.org/).

Corresponding Author: Jun Wang, Peking University People's Hospital, Xi Zhi Men South Avenue No. 11, Beijing, 100044, China. Phone: +86-10-88325952; Fax: +86-10-68349763; E-mail: wangjun@pkuph.edu.cn

Clin Cancer Res 2019;25:7058–67

doi: 10.1158/1078-0432.CCR-19-1213

Translational Relevance

This prospective study showed that the half-life of ctDNA in patients with radical resected lung cancer was just 35 minutes and detection of ctDNA 3 days after surgery is associated with disease-free survival. The result will help with clinical decision making for treating non–small cell lung cancer. First, ctDNA clearance is more rapid than previously reported. Such rapid kinetics confirms that ctDNA levels reflect the rate of active tumor cell death and is a better biomarker for "real-time" reflection of tumor burden in response to therapy. Second, doctors would be able to foreknow the possibility of recurrence before the patient's discharge and plan a precise individualized treatment and follow-up strategy for each patient as early as possible.

metastasis identified by preoperative examination (cStage I–IIIA) and no malignant tumor history within the past 5 years, whose lesions located in lung were not pure ground glass opacity, and neoadjuvant therapy was not performed. The exclusion criteria are as followed: (i) multiple primary lung cancer; (ii) R1, R2 resection during operation; (iii) histology is not non–small cell lung cancer (NSCLC); (iv) negative driver mutation detected in plasma before surgery (time A); (v) germline mutation detected in plasma before surgery (time A); and (vi) unqualified blood samples. The plasma ctDNA concentration was assessed in the patient's plasma at multiple perioperative time points at specific intervals to ensure more accurate data records.

Written informed consent was obtained from each patient for the use of blood and resected tumor tissue for research purposes prior to surgery. This study was approved by Peking University People's Hospital Medical Ethics Committee (2016PHB156-01) in accordance with the Declaration of Helsinki and registered in ClinicalTrials.gov (NCT02965391). The protocol of this study has been published (12).

Surgical technique

Following the long-term treatment of lung cancer, we summarized and optimized our surgical technique (called Wang technique) and published the details of our technique previously (13, 14). All of the patients enrolled in this study were operated on by surgeons who used Wang technique and had achieved proficiency with video-assisted thoracic surgery lobectomy (>200 lobectomies independently) to guarantee the homogeneity of each surgery (15). The time of tumor resection was defined according to the surgery. If the patient had lobectomy directly, the time of pulmonary vein cutoff was considered the time of tumor resection. If the patient underwent tumor wedge resection first, the time was recorded just after wedge resection.

Sample collection

Ten-milliliter plasma samples were obtained immediately before surgery (time A) and at multiple prespecified time points after tumor resection [time B (5 minutes), time C (30 minutes), and time D (2 hours)] and after surgery [time P1 (1 day), time P2 (3 days), and time P3 (1 month), Fig. 1A]. White blood cells from each patient were also collected. Fresh tumor samples were acquired once the perioperative frozen section pathology confirmed NSCLC. At the same time, a normal lung tissue specimen was obtained 2 to 3 cm away from the lesion. The enrolled patients were followed after surgery, and their blood samples were obtained at their postoperative review. Samples at each time point were immediately processed to isolate plasma by double spinning the blood. First, the sample was centrifuged for 10 minutes at 1,600 $\times$ *g*, and peripheral blood lymphocyte debris were stored at -20°C until use. Next, supernatants from these samples were centrifuged at 16,000 $\times$ *g* for 10 minutes, and plasma was collected and stored in 2-mL aliquots at -80°C until needed. At least 4-mL solution of plasma per case was available for this study. cfDNA was extracted from whole plasma within 4 hours. Quality control was performed by spectroscopic analysis. DNA was extracted from tissue and purified plasma samples according to the standard protocol formulated for the DNeasy Blood & Tissue kit (Qiagen) and MagMAX Cell-free DNA Isolation Kit (Applied Biosystems).

DNA sequencing workflow

The circulating single-molecule amplification and resequencing technology (cSMART) is a detection platform based on next-generation sequencing (refs. 16, 17; Fig. 1B). cSMART proceeds through the following steps: labeling, circularization, inverse PCR amplification, high-throughput sequencing, deredundancy, and counting of DNA fragments to determine the ctDNA content in peripheral blood. As previously described (17), DNA libraries were constructed using the total fragmented DNA template extracted from 4 mL of plasma. DNA molecules were end-modified with a 3′ A nucleotide overhang and then ligated with 5′ T-tailed PCR adaptors. Libraries were generated by 15 cycles of PCR using the thermostable proofreading Pfu DNA polymerase (Promega) with a low sequencing error rate of approximately 1 in 105 nucleotides. After denaturation of DNA molecules to single strands, a bridging oligonucleotide synthesized with end sequences complimentary to the PCR adaptors was used to facilitate ligation-mediated circularization with Taq ligase. The bridging oligonucleotide was also specifically designed with a four-based NNNN code and synthesized as a mixture of degenerate molecules, which served to randomly and uniquely bar code every single plasma molecule in the library. Hot spot mutations within the circularized single-strand molecules were then amplified by inverse PCR using primer pairs strategically located 20 to 48 bp from the mutated loci to ensure maximum sensitivity and specificity for mutation detection. A multiplex assay containing a total of 94 inverse primer pairs was used to simultaneously detect and quantitate eight most commonly mutated oncogenic genes with corresponding target therapy options suggested on The National Comprehensive Cancer Network (NCCN) guidelines and one most commonly mutated tumor suppressor gene *TP53* (Supplementary Fig. S1; ref. 18). The pool of allelic molecules generated by inverse PCR was subjected to paired-end sequencing on the NextSeq 500 platform (Illumina). The publicly available FASTQ-join program (https://expressionanalysis.github.io/ea-utils) was then used to reconstruct the overlapping paired-end sequences to generate contiguous consensus sequences for each allelic molecule (19). A minimum of one unique read was used to define a read group with or without a mutation. Duplicate or higher order reads with the same start and stop positions were distinguished by their unique bar codes and counted only once to correct for PCR bias. All mutant molecules meeting these quality control criteria were counted. The abundance of each mutation

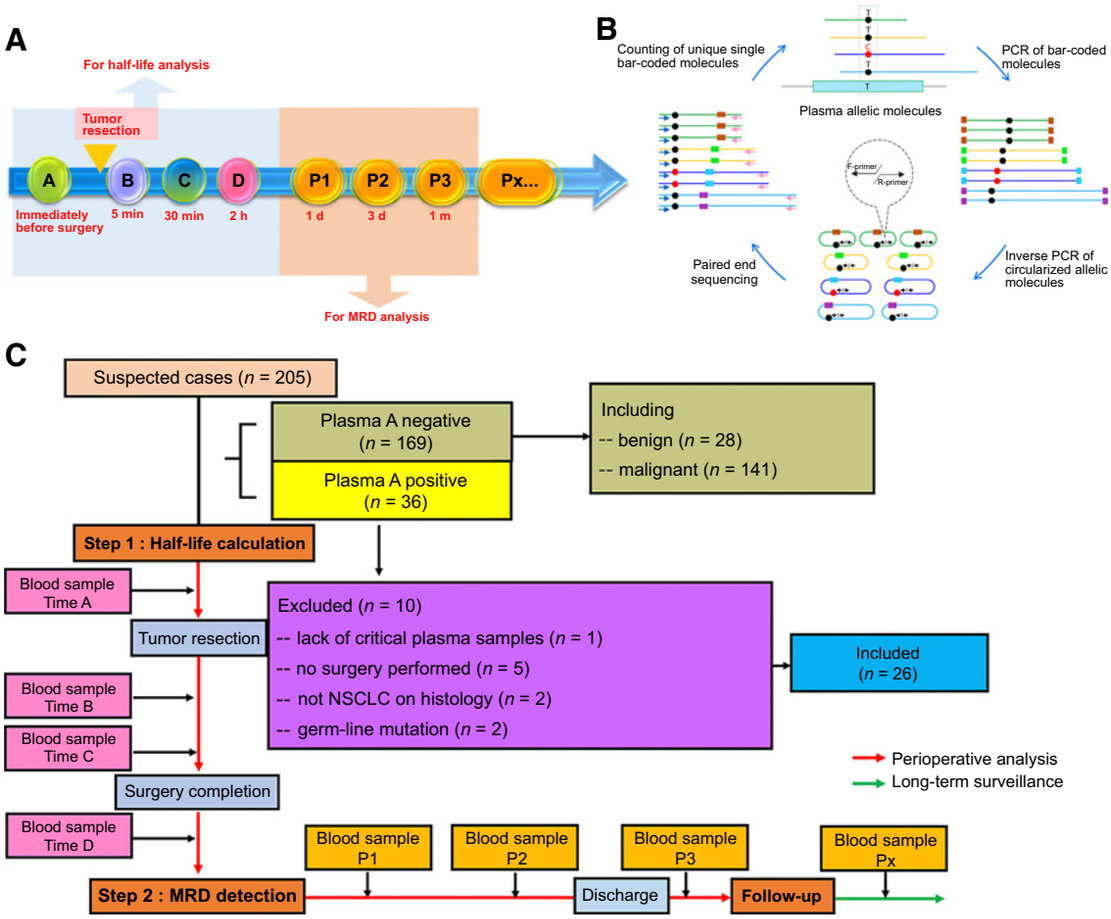

Figure 1.

Overview of prespecified biopsies and CONSORT diagram describing the DYNAMIC study. **A,** Prespecified blood time points, ctDNA from time A to time D are for half-life analysis, whereas time P1, time P2, time P3 for MRD detection. The actual blood collection time is based on these prespecified time points and are shown in Supplementary Table S5. **B,** Concept of cSMART for quantification of allelic variants in plasma. Single allelic molecules (colored lines) were identified by their unique bar codes (colored boxes) and/or unique start/stop sequences. Targeted molecules were sequenced, and unique molecules were counted to determine allelic ratios in the original plasma. **C,** Study profile. Thirty-six patients showed detectable mutations in plasma A. Two were excluded after validation with tumor tissue and normal lung tissue showing a CHIP. One was small cell lung cancer and one was carcinosarcoma. One patient who lacked plasma samples at too many time points plasma samples and 5 patients who did not receive curative surgery were also excluded. Finally, 26 patients were included in this study.

was expressed as the mutation ratio of mutant and total molecule numbers per 4 mL of plasma, which could be used for monitoring changes in the plasma mutation level before or after surgery. The known mutations specifically targeted in this study were G719A/C/S (three variants, G719X), exon 19 deletions (16 variants), exon 20 insertions (three variants), S768I, T790M, C797S, and exon 21 point mutations L858R and L861Q in EGFR; G12A/C/D/R/S/V (six variants, G12X), G13D, Q61E/H/K/L/P/R (six variants, Q61X), and A146T/P/V (three variants, A146X) in KRAS; exon 20 insertions (five variants) in ERBB2; V600D/E/K/R (four variants, V600X) in BRAF; R88Q, E542K, E545K/D (two variants, E545X), and A1047R/L (two variants, A1047X) in PIK3CA; R175C/H (two variants, R175X), R248W/Q (two variants, R248X), and R273C/H (two variants, R273X) in TP53; MET exon 14 skipping; and ALK/RET fusions (12). Mutations other than the hot spots listed above but within the nearby region picked up by the primers were also reported.

Methodology and tech features

In cSMART assay, each cfDNA molecule is uniquely bar-coded with specially designed short adapters and universally amplified to make duplicates of the original molecule. The amplification products are circularized and reamplified with target-specific back-to-back primer pair pools to enrich the targets. This unique primer design makes the target sequences amplified inversely and therefore preserved the molecular bar codes and the length information of the original cfDNA molecule. The inversely amplified DNA products are then ligated with Illumina TruSeq adapter and sequenced to 150 base pairs from each end at very high depth (>20,000×) with Illumina NextSeq 500. The original cfDNA molecules are reconstituted by a multistep bioinformatics pipeline, during which the sequencing errors are corrected according to the consensuses from the bar-coded duplicates. These reconstituted molecules are counted, and the mutant allele frequencies are calculated.

cSMART assay utilizes multiplexed inverse PCR technology, which is similar to conventional amplicon sequencing methods (20). However, the inverse PCR technology enables the assay to preserve the molecular bar codes and the DNA end information of the original cfDNA molecule. These features are commonly found in hybrid capture methods but rarely in amplicon sequencing technologies and make cSMART assay much more sensitive and suitable for ctDNA detection.

For each enrolled patient, both tumor tissue and ctDNA were detected by cSMART sequencing and data analysis. Some mutations that lead to clonal expansion but do not result in hematologic malignancies are referred to as clonal hematopoiesis of undetermined potential (CHIP; ref. 11). These cfDNA mutations lead to false positives for MRD detection. Therefore, we also sequenced white blood cells and normal tissue concurrently to filter out CHIP-related mutations.

Limit of detection

cSMART assay requires 4-mL plasma from the patient's peripheral blood and utilizes all the cfDNA extracted. Therefore, the limit of detection (LOD) of cSMART assay varies depending on the amount of the input cfDNA. The median cfDNA yield from 4-mL plasma of a patient with cancer is 46.9 ng ($n = 3182$). With patients who have a higher cfDNA yield than 50 ng as input, the LOD on mutation allele frequency (MAF) is 0.01%, as tested with synthetic cfDNA reference standards (for SNV and indels, LOD was tested with HD825 from HDx; for fusions, LOD was tested with homemade reference standards verified by ddPCR).

Statistical analysis

The plasma MAF at each time point was calculated, and the ctDNA concentration was calculated by multiplying the MAF by the cell-free DNA concentration. Previous studies have shown that circulating virus (Epstein-Barr virus) DNA and fetal DNA decline exponentially in the circulation (8, 9). Therefore, in this study, we hypothesized that the decline of ctDNA in patients with NSCLC is consistent with an exponential decay model; after the natural logarithm of the plasma ctDNA MAF was plotted against time, a straight line with a slope of K and coefficient of correlation R^2 were obtained by linear regression. The half-life was determined using the equation: half-life = 0.693/K. Perioperative time-points from time A (before surgery) to time D (2 hours after tumor resection) were selected for half-life calculation. Considering the effects of intraoperative surgical processes on the ctDNA MAF, the half-life was calculated when the ctDNA MAF reached a maximum value until the last nonzero level.

OS was defined as the time between the surgery date and patient death resulting from cancer-related cause. Recurrence-free survival (RFS) was defined as the time from the date of surgery until the onset of relapse, metastasis, or death from any cause. MRD landmark was defined from 1 day (P1) after operation to 1 month (P3). When multiple mutations were assessed, ctDNA was defined as positive if any of the mutations was positive. The survival curves were plotted using the Kaplan–Meier method. Linear regression and the half-life calculation were performed using SigmaStat 2.0 software. Statistical analysis of the data was performed using SPSS 22.0 software.

Results

Between November 2016 and September 2017, 205 consecutive patients with suspected lung cancer received preoperative blood mutation tests (intent-to-treat population; Fig. 1C). Thirty-six of these patients showed detectable mutations in time A. Relationship between clinicopathologic factors and plasma ctDNA detection (time A) was shown in Table 1. Multivariable analysis indicated that tumor size and lymph node invasion were independent predictors of ctDNA detection (Fig. 2A). Tumor maximum square correlated with the amount of ctDNA in plasma (pg/mL; Spearman $\rho = 0.781$, $P < 0.001$; Fig. 2B and C).

Twenty-six patients who received curative resections with positive plasma A were enrolled finally. The clinical features

Table 1. Relationship between clinicopathologic factors and plasma mutation status in time A

	Positive in time A ($n = 32$)	Negative in time A ($n = 143$)	*P*
Age (y)[a]	63 (15)	63 (15)	0.744
Gender			0.051
Male	22 (68.7%)	70 (49.0%)	
Female	10 (31.3%)	73 (51.0%)	
Smoke history			**0.000**
Positive	23 (71.9%)	47 (32.9%)	
Negative	9 (28.1%)	96 (67.1%)	
Location[b]			0.257
Right upper lobe	9 (28.1%)	44 (30.8%)	
Right medium lobe	1 (3.1%)	11 (7.7%)	
Right lower lobe	10 (31.2%)	22 (15.3%)	
Left upper lobe	6 (18.8%)	26 (18.2%)	
Left lower lobe	6 (18.8%)	40 (28.0%)	
Maximum diameter of tumor (cm)[c]			**0.000**
≤3	6 (19.7%)	101 (70.6%)	
>3	26 (81.3%)	42 (29.4%)	
Pathology			**0.003**
Adenocarcinoma	17 (53.1%)	115 (80.4%)	
Nonadenocarcinoma	15 (46.9%)	28 (19.6%)	
Lymph node invasion			**0.000**
Negative	12 (37.5%)	111 (77.6%)	
Positive	20 (62.5%)	32 (22.4%)	
N2-negative	8 (40.0%)	13 (40.6%)	
N2-positive	12 (60.0%)	19 (59.4%)	
pTNM stage			**0.000**
I	3 (9.4%)	97 (67.8%)	
II	8 (25.0%)	22 (15.4%)	
III and above	21 (65.6%)	24 (16.8%)	
Pleural invasion			0.217
Positive	15 (46.9%)	46 (32.2%)	
Negative	17 (53.1%)	97 (67.8%)	
Peritumor intravascular cancer emboli			**0.005**
Positive	21 (65.6%)	51 (35.7%)	
Negative	11 (34.4%)	92 (64.3%)	

Boldface indicates the following: Chi-square test/Fisher's exact test and Mann-Whitney U test were used for categorical variables and for continuous variables, respectively. *P* values shown reflect comparison between patients with positive ctDNA in time A and patients with negative ctDNA in time A. *P* values < 0.05 were considered significant.

Abbreviation: pTNM, pathological tumor–node–metastasis.

[a]Data do not meet the normal distribution and the data are described by the median (interquartile range).

[b]There were a few tumors that invaded multiple lung lobes simultaneously.

[c]Two patients with non-NSCLC with positive plasma A were excluded. Two positive plasma A patients with CHIP were analyzed in the negative group.

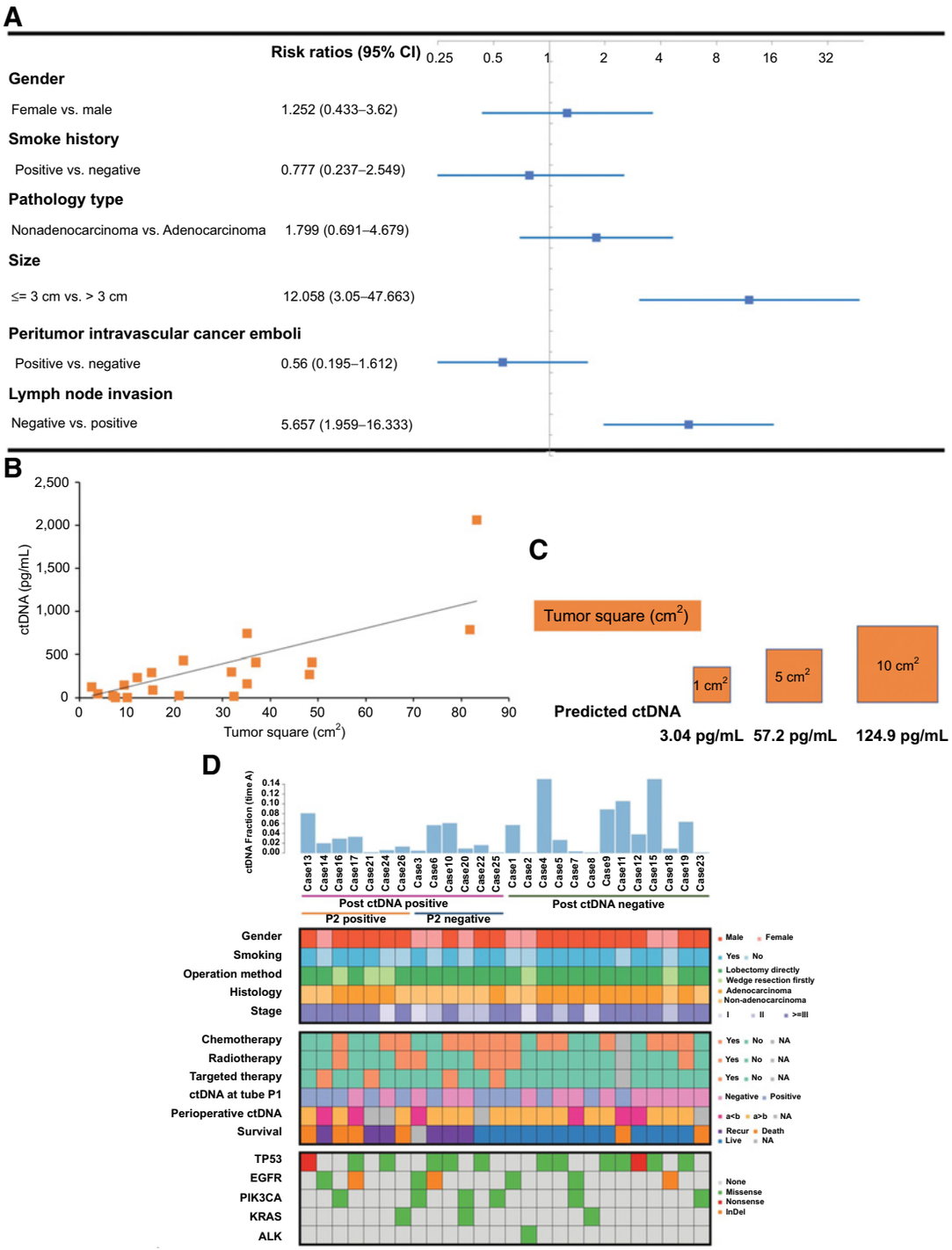

Figure 2.

ctDNA detection. **A,** Multivariable logistic analysis of relationship between clinicopathologic factors and plasma mutation status at time A. **B,** Tumor square (cm^2) measured by CT correlates with the amount of ctDNA in plasma (pg/mL). A linear relationship was observed. **C,** The predicted amount of ctDNA at hypothetical square ranging from 1 cm^2 to 10 cm^2 is based on the model in **B**. 10-mL plasma contained about 100-ng cfDNA in this study (Supplementary Table S6), a maximum square of 1-cm^2 tumor in CT scan would be estimated to a mean clonal plasma MAF of 0.03%. **D,** Clinicopathologic features and genetic variation detection data. Each column represents data from a single patient. CI, confidence interval.

of the patients are shown in Fig. 2D and Supplementary Table S1. Five patients detected concomitant mutations. The positive concordance between plasma and tissue is 92.9% (26/28). The overall concordance rate of all mutations is 83.9% (26/31). The specific amino acid changes in each gene in tumor and matched plasma are shown in Supplementary Figs. S2 and S3.

In most cases, the plasma ctDNA concentration showed a rapid decreasing trend over time. Three cases (cases 2, 8, and 12) showed rapid clearance to zero once the plasma ctDNA concentrations reached a maximum value and were excluded from the half-life analysis; in addition, another six cases (cases 21–26) were excluded because of incomplete perioperative blood samples. The dynamic changes in the ctDNA concentrations of the remaining 17 patients from times A to D are summarized in Fig. 3A. The average plasma ctDNA MAF for times A, B, C, and D was 2.72%, 2.11%, 1.14%, and 0.17%, respectively (Fig. 3B). The plasma ctDNA concentrations of six patients showed transient increases at time B and then decreased gradually thereafter. In each patient, the natural logarithm of the plasma ctDNA MAF was plotted against time, as shown in Fig. 3C. The median R^2 of each curve was 0.95 (interquartile range, 0.14; nonnormal distribution), and the linearity of the plots supports the exponential decay model. The median ctDNA half-life was 35 minutes (8–147 minutes). The detailed linear regression formula of each patient, plasma ctDNA concentrations, and curves at each time point during the perioperative period are shown in Supplementary Tables S2 and S3 and Supplementary Fig. S4. Considering there were five cases containing two mutations simultaneously in plasma ctDNA, we calculate each mutation separately to analyze the relationship between ctDNA half-life and clinical characteristics, a total of 21 curves were included. Different mutations in the same patient showed similar clearance pattern, as shown in Supplementary Fig. S4. Patients with MRD detection had a significant slower ctDNA half-life than those with negative MRD (103.2 minutes vs. 29.7 minutes, $P = 0.001$). The result showed that there were no clinical features affecting the ctDNA clearance rate in blood (Fig. 3D).

All the 26 patients received postoperative follow-up with plasma ctDNA monitoring, and the median follow-up time was 532 days (480–682 days) in all patients and 629 days (567–718 days) in patients who were free from progression. The detailed longitudinal ctDNA profiles of these patients are presented in Supplementary Fig. S5. Detection of ctDNA from time P1 (1 day), time P2 (3 days), and time P3 (1 month, three cases with no blood samples at this time point were excluded) determined the most appropriate time for MRD detection. There were no clinical features that influenced the plasma ctDNA concentration at time P1, P2, and P3 (Supplementary Table S4). The actual blood collection time is based on prespecified time points and is shown in Supplementary Table S5. Among the 12 patients whose plasma ctDNA concentrations were not 0% at time P1, five (cases 6, 13, 14, 16, and 21) had recurrences, one (case 13) died from cancer, two (cases 11 and 26) died because of a non–cancer-related cause, and five (cases 1, 4, 8, 22, and 25) had their plasma ctDNA concentrations dropped to 0% at time P2 and kept 0% at time P3 having good prognosis. While at time P2, seven patients (cases 13, 14, 16, 17, 21, 24, and 26) had detectable ctDNA concentrations, six of whom (85.7%) suffered relapse. No patients with detectable ctDNA at time P2 converted to negative at time P3. The average RFS of patients with detectable and undetectable ctDNA concentrations at time P1 was 528 days and 543 days, respectively ($P = 0.657$), whereas at time P2 was 278 days and 637 days, respectively ($P = 0.002$), and at time P3 was 295 days and 662 days, respectively ($P = 0.003$). In case 17, the plasma ctDNA concentration decreased to 0% at time P1 and rebounded to 0.02% at time P2 and 1.94% at time P3. This patient relapsed on the 47th day after surgery, and the plasma ctDNA concentration rose to 3.44%. The average OS times were 605 days and 657 days for patients with detectable and undetectable ctDNA at time P1, respectively ($P = 0.462$), whereas at time P2 were 434 days and 720 days, respectively ($P = 0.018$) and at time P3 were 476 days and 717 days, respectively ($P = 0.045$; Fig. 4; Supplementary Fig. S6). Fifteen patients maintained negative ctDNA levels throughout the course of monitoring and 14 of these patients showed good prognosis. Like case 9, although the CT scan showed suspected tumor relapse 6 months after surgery, the mass was finally considered inflammation and presented a concordance with the ctDNA finding (Fig. 4G). Only 1 ctDNA-negative patient experienced recurrence. The median lead time for detection of tumor recurrence by ctDNA rather than by CT was 165 days (12–337 days). Seventeen patients underwent adjuvant therapy after surgery, including 14 cases of postoperative chemotherapy, seven cases of postoperative radiotherapy, and four cases of targeted therapy. For patients with positive ctDNA at time P2, the RFS of those who had received adjuvant therapy was 269 days whereas the RFS of those who did not was 111 days, $P = 0.018$ (Supplementary Fig. S7). The ctDNA changes were correlated with treatment response (Fig. 4H).

Discussion

The DYNAMIC study reveals the rapid clearance of ctDNA in patients with lung cancer and the appropriate time for ctDNA analysis to detect MRD in surgical patients with lung cancer. To the best of our knowledge, this is the first prospective cohort study to show perioperative dynamic changes in ctDNA in any patients with cancer and to investigate the appropriate time for applying the ctDNA approach for MRD detection.

The ctDNA detection rate is 19.2% (34/177) in this prospective cohort study. The relatively lower sensitivity is due to the following reasons. First, most enrolled patients had lung adenocarcinoma [75.4% (132/175)]. TRACERx study has shown that histology is one of the predictors of ctDNA detection in early-stage NSCLC, in which the positive percentage of ctDNA in lung adenocarcinomas was just 19% (11/58; ref. 4). Second, previous study has shown that the sensitivity of SNV ctDNA detection is constrained by tumor size using current technologies. Tumor of 10 cm^3 equates to a mean plasma MAF of clonal alterations of 0.1% (11). Because the majority of the tumor size in our study was less than 3 cm [61.1% (107/175)], combining with the histology in this cohort, the detection rate is reasonable. In addition, this study is the first to reveal the correlation between tumor maximum square (which is easy to obtain by CT scan than tumor volume) with the amount of ctDNA in plasma. The result suggests that the low tumor cell burden will limit our capacity to detect the smallest stage I lung cancer using current ctDNA approaches, which confirmed the TRACER study's result from the Asian patients (11).

Except the few observational studies focusing on circulating virus DNA and circulating fetal DNA that have shown the half-

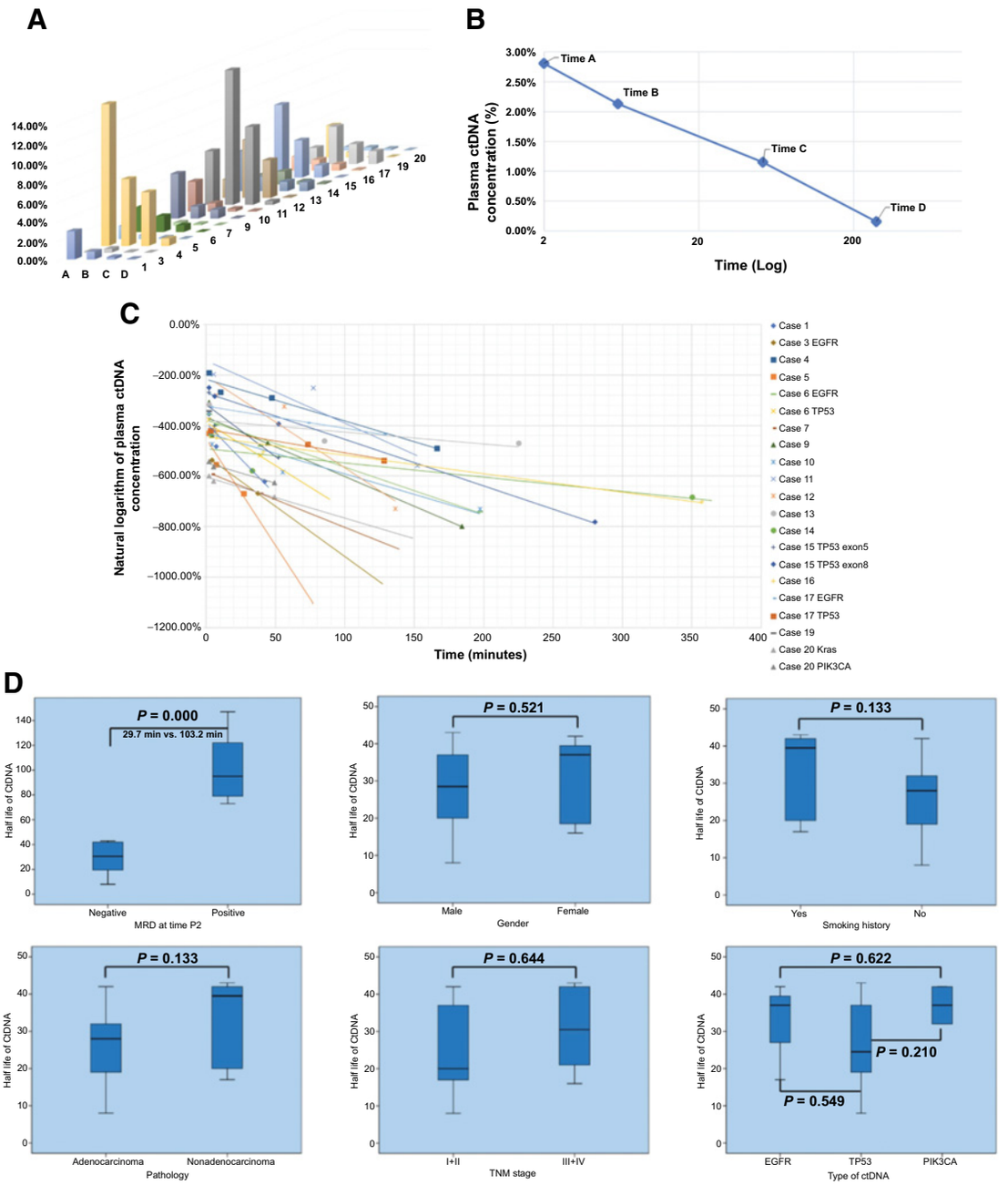

Figure 3.

Half-life analysis of plasma ctDNA decay. **A,** The plasma ctDNA concentration from time A to time D in patients was subjected to a half-life calculation. **B,** The average ctDNA concentration from time A to D. **C,** The natural logarithm of the plasma ctDNA concentration (*y*-axis) is plotted against time (*x*-axis) for the period from the peak concentration to the last nonzero time point. **D,** Clinical features affecting the ctDNA clearance rate in blood. Patients with time P2 MRD detection had a significant slower ctDNA half-life than those with negative MRD (103.2 minutes vs. 29.7 minutes, $P = 0.000$). There were no clinical features (gender, smoke history, pathology, ctDNA type, and TNM stage) affecting the rate of ctDNA clearance in blood.

life of circulating DNA in blood decay rapidly in human circulation (9, 21), little data are available on the stability of ctDNA in patients with cancer. Whether these results can be generalized to other solid tumors is unknown (22). The only study for half-life of ctDNA was conducted by Diehl and colleagues, in which from only one patient with stage IV colorectal cancer whose plasma was sampled at four time points after complete resection, they estimated the half-life of ctDNA after surgery to be 114 minutes (7). However, the time points that the authors selected were much distant from this time. In addition, we cannot assess the ctDNA half-life in late-stage patients because residue tumor definitely exists in these

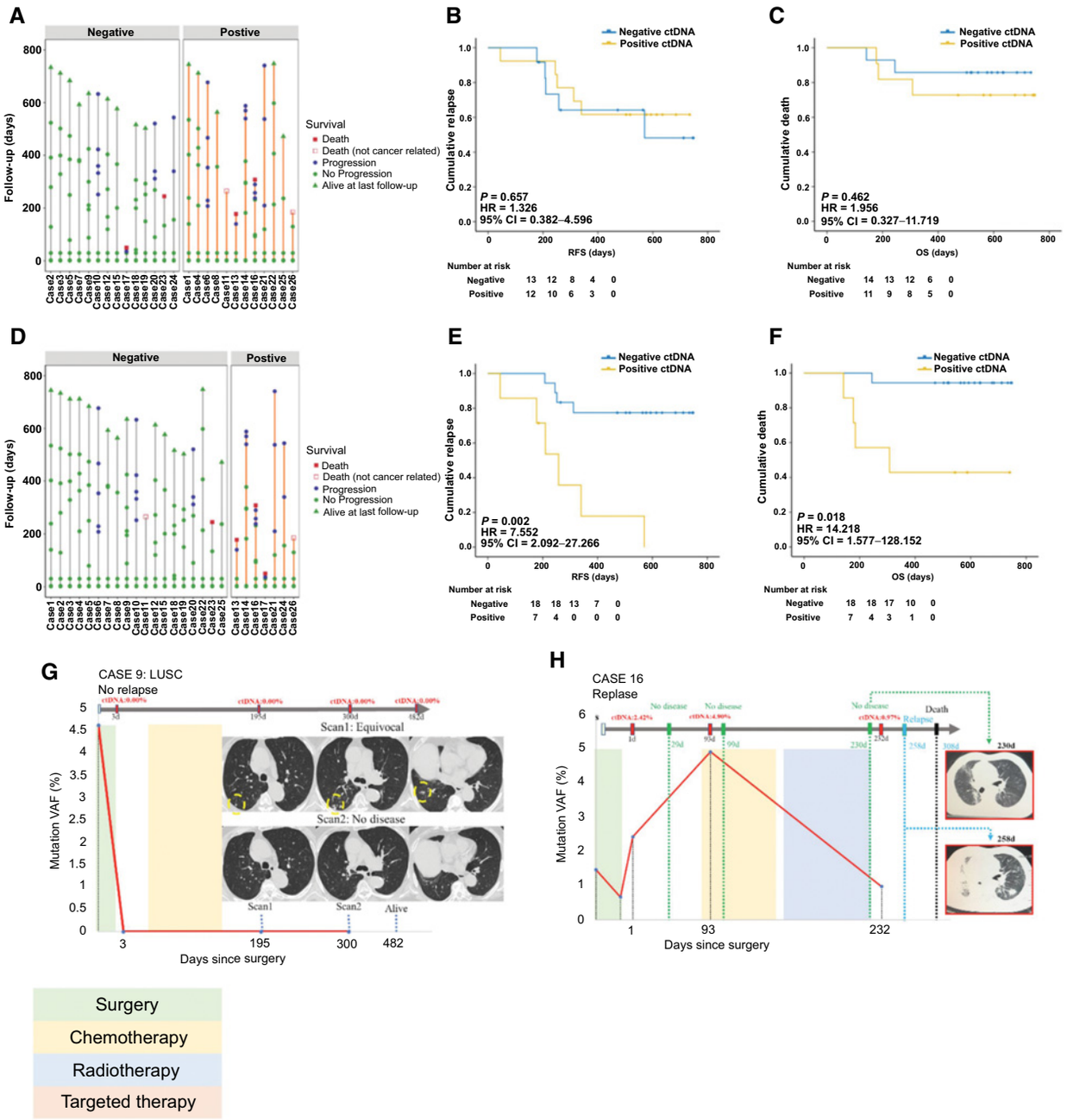

Figure 4.

Detection of MRD and survival analysis at time P1 and P2. **A,** Survival of patients with detected and undetected ctDNA at time P1 surveillance. RFS (**B**) and OS (**C**) between different ctDNA statuses at time P1. **D,** Survival of patients with detected and undetected ctDNA at time P2 surveillance. RFS (**E**) and OS (**F**) between different ctDNA statuses at time P2. Progression was evaluated by RECIST 1.1 criteria. Kaplan–Meier survival curve according to different ctDNA statuses during postoperative monitoring. **G,** Longitudinal ctDNA profile of case 9 LUSC patient with false-positive imaging. **H,** Longitudinal ctDNA profile of case 16. The patient was treated with chemotherapy 79–131 days after surgery and radiotherapy 162–204 days after surgery. ctDNA changes were correlated with treatment response. CI, confidence interval; LUSC, lung squamous cell carcinoma; VAF, variant allele frequency.

patients. Therefore, the accurate elimination rate of ctDNA in patients with cancer remained undetermined. We prospectively incorporated a series of subtle time points (A–D) that were within 2 hours of tumor resection into the ctDNA half-life calculation. The results showed that the precise half-life in surgical patients with lung cancer was approximately 35 minutes. The median coefficient of correlation R^2 was 0.95, which verified the reliability of our result. Although how metabolism and physiologic changes contribute to ctDNA clearance is not entirely understood, the half-life of ctDNA is more rapid than

previously reported as about 2 hours (7) and seems to have no correlation with clinical characteristics and genetic variants. Such rapid kinetics confirms that ctDNA levels reflect the rate of active tumor cell death and are a better biomarker for "real-time" reflection of tumor burden in response to therapy comparing with other relatively slow clearance rate blood markers (2). All the six patients showing transient increase at time B than time A underwent lobectomy directly. Because lobectomy may require repeatedly moving the pulmonary lobe than wedge resection, the increase in ctDNA is probably due to the perioperative active rapid release of tumor cells or cellular secretions into the circulation during surgery. Similar up-and-down fluctuating curves were also observed for circulating virus DNA in patients with nasopharyngeal carcinoma who underwent radiotherapy (21), and studies investigate the short-term changes of ctDNA levels after the initiation of immunotherapy (23), demonstrating the instant monitoring capability of ctDNA.

Although ctDNA detection may be useful for monitoring MRD after surgery, no standard time for postoperative plasma ctDNA detection was established (5, 24); whether the detection of ctDNA after surgery is due to MRD or incomplete vanishment is unclear. We compared plasma samples 1 day (P1), 3 days (P2), and 1 month (P3) after tumor resection and found that P2 and P3 were more related to tumor recurrence. At time P1, all five patients with positive ctDNA whose plasma ctDNA concentrations dropped to 0% at time P2 had good prognoses during follow-up, and MRD detection at 1 day after surgery may have been confounded by incompletely degraded ctDNA. Although ctDNA shows rapid clearance in plasma, false positivity caused by the persistence of ctDNA may occur if we obtained plasma for surveillance too early after surgery. Although time P3 showed similar results with time P2 in MRD detection, patients are most likely discharged from the hospital at time P3 and may be lost to follow-up afterward. Studies based on large database in the United States, Europe, and Asia have shown that the average hospital length of stay is 3 to 10 days for patients with resected NSCLC (13, 25–27); MRD detection would be more practical and meaningful at the 3-day time point because doctors would be able to obtain a sample to determine the possibility of recurrence before the patient leaves the hospital and plan a precise individualized treatment and follow-up strategy for each patient as early as possible. In addition, a later time point such as 1 month or 2 months after surgery may be confused by patients who have early tumor recurrence, as case 17 in this study, who had a relapse at 47 days after surgery.

The potential ability of ctDNA to detect occult cancer and to track tumor-specific mutations lends itself naturally toward assessment of MRD. Most of these studies were retrospective and did not focus on surgically treated patients. Chaudhuri and colleagues retrospectively analyzed ctDNA detection for MRD from 40 patients with stage I–III lung cancer who were mostly treated with radiotherapy (5). The only prospective study that focused on surgical patients was the TRACERx clinical trial, which used mutiplex PCR to detect ctDNA after whole-exome sequencing of tumor tissue, showing that ctDNA was detected in 92.9% of relapse cases 70 days prior to clinical CT scan confirmation (4). This patient-specific assay panel is limited by cost and time, making its wide use in clinical practice inconvenient. Similar to the TRACERx study, our long-term follow-up data also presented the feasibility of longitudinal ctDNA monitoring for tumor relapse in patients with R0 resected lung cancer. We also showed a preliminary result that similar to tumor–node–metastasis system stage, therapy based on ctDNA MRD detection, can contribute to longer survival (Supplementary Fig. S7), but this result should be interpreted by caution because of the small sample size. Before routine clinical application, studies need to investigate whether this strategy can contribute to improved outcomes (28, 29). Next step of clinical trial should be designed to randomize patients treated with present standard management or treatment based on ctDNA detection (30, 31).

There are some limitations in this study. First, a more comprehensive and gene panel may increase the detection rate of ctDNA than just tracking a targeted driver variation panel. However, the main goal of this study was to investigate the accurate half-life of ctDNA. These common driver mutations usually present as clonal mutations with a high allele frequency (11). Although a larger panel may increase the detection sensitivity, tracking low-frequency subclonal mutations cannot contribute to the assessment of the elimination rate of ctDNA because such lower value may lead to a larger error in accurate calculation. Second, there is only 30 to 200 ng of cfDNA in a 10-mL blood sample from patients with cancer (11, 32). Because increasing the volume of blood collected (e.g., 20 mL instead of 10 mL) from patients to increase sensitivity would be inappropriate, a more sensitive approach incorporating multiomics-like methylation, exosomes, circulating miRNA, metabonomics, and/or molecular imaging methods could detect ctDNA at lower thresholds with greater accuracy and provide more practical value for MRD detection (10). Finally, larger sample size studies should be performed to further validate ctDNA MRD detection in surveillance. We are performing a large prospective study (NCT03634826) with 200 patients to systematically evaluate and compare the detection of aberrant methylation and SNV in ctDNA among surgical patients with NSCLC, aiming to define effective strategies for postoperative surveillance by integrating genetic and epigenetic information of ctDNA (3).

In summary, this is the first prospective study to evaluate perioperative dynamic changes in ctDNA in patients with primary lung cancer. For patients with surgical lung cancer, ctDNA decays rapidly after tumor resection. Three days after surgery can be used as the base value for lung cancer postoperative surveillance and is convenient to inform clinical decision making. Future clinical trials are needed to determine whether blood-based MRD detection can result in an OS benefit.

Disclosure of Potential Conflicts of Interest

No potential conflicts of interest were disclosed.

Authors' Contributions

Conception and design: K. Chen, L.T. Wang, J. Wang
Development of methodology: K. Chen, H. Zhao, L.T. Wang
Acquisition of data (provided animals, acquired and managed patients, provided facilities, etc.): H. Zhao, G. Kang, Y. Nie
Writing, review, and/or revision of the manuscript: K. Chen, H. Zhao
Analysis and interpretation of data: K. Chen, H. Zhao, Y. Shi
Administrative, technical, or material support (i.e., reporting or organizing data, constructing databases): F. Yang, G. Kang
Study supervision: F. Yang, L.T. Wang, J. Wang

Other (trial physician on this study and involved in patient recruitment): K. Chen, H. Zhao
Other (trial manager for administration of the study): K. Chen, J. Wang

Acknowledgments

We acknowledge the contributions of Yun Wang, Yanyan Hou, Dr. Kaize Zhong, and Dr Qi Huang of Peking University People's Hospital for assistance with sample collection and reservation. We also thank the patients and their families and staff members at all study sites who enrolled and helped with this trial.

This study was supported by the National Natural Science Foundation of China (No. 81602001, to K. Chen) and National Natural Science Foundation of China (No. 81772469, to F. Yang).

The costs of publication of this article were defrayed in part by the payment of page charges. This article must therefore be hereby marked *advertisement* in accordance with 18 U.S.C. Section 1734 solely to indicate this fact.

Received April 18, 2019; revised May 31, 2019; accepted August 19, 2019; published first August 22, 2019.

References

1. Corcoran RB, Chabner BA.Application of cell-free DNA analysis to cancer treatment. N Engl J Med 2018;379:1754–65.
2. Siravegna G, Marsoni S, Siena S, Bardelli A. Integrating liquid biopsies into the management of cancer. Nat Rev Clin Oncol 2017;14:531–48.
3. Chen K, Kang G, Zhao H, Zhang K, Zhang J, Yang F, et al. Liquid biopsy in newly diagnosed patients with locoregional (I-IIIA) non-small cell lung cancer. Expert Rev Mol Diagn 2019;19:419–27.
4. Abbosh C, Birkbak NJ, Wilson GA, Jamal-Hanjani M, Constantin T, Salari R, et al. Phylogenetic ctDNA analysis depicts early-stage lung cancer evolution. Nature 2017;545:446–51.
5. Chaudhuri AA, Chabon JJ, Lovejoy AF, Newman AM, Stehr H, Azad TD, et al. Early detection of molecular residual disease in localized lung cancer by circulating tumor DNA profiling. Cancer Discov 2017;7:1394–403.
6. Diaz LA Jr, Bardelli A. Liquid biopsies: genotyping circulating tumor DNA. J Clin Oncol 2014;32:579–86.
7. Diehl F, Schmidt K, Choti MA, Romans K, Goodman S, Li M, et al. Circulating mutant DNA to assess tumor dynamics. Nat Med 2008;14: 985–90.
8. Lo YM, Leung SF, Chan LY, Chan AT, Lo KW, Johnson PJ, et al. Kinetics of plasma Epstein-Barr virus DNA during radiation therapy for nasopharyngeal carcinoma. Cancer Res 2000;60:2351–5.
9. Lo YM, Zhang J, Leung TN, Lau TK, Chang AM, Hjelm NM. Rapid clearance of fetal DNA from maternal plasma. Am J Hum Genet 1999; 64:218–24.
10. Wan JCM, Massie C, Garcia-Corbacho J, Mouliere F, Brenton JD, Caldas C, et al. Liquid biopsies come of age: towards implementation of circulating tumour DNA. Nat Rev Cancer 2017;17:223–38.
11. Abbosh C, Birkbak NJ, Swanton C. Early stage NSCLC—challenges to implementing ctDNA-based screening and MRD detection. Nat Rev Clin Oncol 2018;15:577–86.
12. Chen K, Zhao H, Yang F, Hui B, Wang T, Wang LT, et al. Dynamic changes of circulating tumour DNA in surgical lung cancer patients: protocol for a prospective observational study. BMJ Open 2018;8:e019012.
13. Chen K, Wang X, Yang F, Li J, Jiang G, Liu J, et al. Propensity-matched comparison of video-assisted thoracoscopic with thoracotomy lobectomy for locally advanced non-small cell lung cancer. J Thorac Cardiovasc Surg 2017;153:967–76.
14. Sullivan R, Alatise OI, Anderson BO, Audisio R, Autier P, Aggarwal A, et al. Global cancer surgery: delivering safe, affordable, and timely cancer surgery. Lancet Oncol 2015;16:1193–224.
15. Li X, Wang J, Ferguson MK. Competence versus mastery: the time course for developing proficiency in video-assisted thoracoscopic lobectomy. J Thorac Cardiovasc Surg 2014;147:1150–4.
16. Lv W, Wei X, Guo R, Liu Q, Zheng Y, Chang J, et al. Noninvasive prenatal testing for Wilson disease by use of circulating single-molecule amplification and resequencing technology (cSMART). Clin Chem 2015;61: 172–81.
17. Wang Z, Cheng G, Han X, Mu X, Zhang Y, Cui D, et al. Application of single-molecule amplification and resequencing technology for broad surveillance of plasma mutations in patients with advanced lung adenocarcinoma. J Mol Diagn 2017;19:169–81.
18. Ettinger DS, Wood DE, Aisner DL, Akerley W, Bauman J, Chirieac LR, et al. Non-small cell lung cancer, version 5.2017, NCCN clinical practice guidelines in oncology. J Natl Compr Canc Netw 2017;15:504–35.
19. Aronesty E.Comparison of sequencing utility programs. Open Bioinformatics J 2013;7:1–8.
20. Chen KZ, Lou F, Yang F, Zhang JB, Ye H, Chen W, et al. Circulating tumor DNA detection in early-stage non-small cell lung cancer patients by targeted sequencing. Sci Rep 2016;6:31985.
21. To EW, Chan KC, Leung SF, Chan LY, To KF, Chan AT, et al. Rapid clearance of plasma Epstein-Barr virus DNA after surgical treatment of nasopharyngeal carcinoma. Clin Cancer Res 2003;9:3254–9.
22. Heitzer E, Ulz P, Geigl JB. Circulating tumor DNA as a liquid biopsy for cancer. Clin Chem 2015;61:112–23.
23. Goldberg SB, Narayan A, Kole AJ, Decker RH, Teysir J, Carriero NJ, et al. Early assessment of lung cancer immunotherapy response via circulating tumor DNA. Clin Cancer Res 2018;24:1872–80.
24. Yu SC, Lee SW, Jiang P, Leung TY, Chan KC, Chiu RW, et al. High-resolution profiling of fetal DNA clearance from maternal plasma by massively parallel sequencing. Clin Chem 2013;59:1228–37.
25. Boffa DJ, Dhamija A, Kosinski AS, Kim AW, Detterbeck FC, Mitchell JD, et al. Fewer complications result from a video-assisted approach to anatomic resection of clinical stage I lung cancer. J Thorac Cardiovasc Surg 2014;148:637–43.
26. Falcoz PE, Puyraveau M, Thomas PA, Decaluwe H, Hürtgen M, Petersen RH, et al. Video-assisted thoracoscopic surgery versus open lobectomy for primary non-small-cell lung cancer: a propensity-matched analysis of outcome from the European Society of Thoracic Surgeon database. Eur J Cardiothorac Surg 2016;49:602–9.
27. Yang CF, Sun Z, Speicher PJ, Saud SM, Gulack BC, Hartwig MG, et al. Use and outcomes of minimally invasive lobectomy for stage I non-small cell lung cancer in the national cancer data base. Ann Thorac Surg 2016;101: 1037–42.
28. Merker JD, Oxnard GR, Compton C, Diehn M, Hurley P, Lazar AJ, et al. Circulating tumor DNA analysis in patients with cancer: American Society of Clinical Oncology and College of American Pathologists joint review. J Clin Oncol 2018;36:1631–41.
29. Wang Z, Cheng Y, An T, Gao H, Wang K, Zhou Q, et al. Detection of EGFR mutations in plasma circulating tumour DNA as a selection criterion for first-line gefitinib treatment in patients with advanced lung adenocarcinoma (BENEFIT): a phase 2, single-arm, multicentre clinical trial. Lancet Respir Med 2018;6:681–90.
30. Yang M, Forbes ME, Bitting RL, O'Neill SS, Chou PC, Topaloglu U, et al. Incorporating blood-based liquid biopsy information into cancer staging: time for a TNMB system? Ann Oncol 2018;29:311–23.
31. Chae YK, Oh MS.Detection of minimal residual disease using ctDNA in lung cancer: current evidence and future directions. J Thorac Oncol 2019; 14:16–24.
32. Szpechcinski A, Chorostowska-Wynimko J, Struniawski R, Kupis W, Rudzinski P, Langfort R, et al. Cell-free DNA levels in plasma of patients with non-small-cell lung cancer and inflammatory lung disease. Br J Cancer 2015;113:476–83.